Metal Oxide Nanoassemblies

DOI: 10.1002/anie.200800431

Supramolecular Metal Oxides: Programmed Hierarchical Assembly of a Protein-Sized 21 kDa $[(C_{16}H_{36}N)_{19}\{H_2NC(CH_2O)_3P_2V_3W_{15}O_{59}\}_4]^{5-}$ Polyoxometalate Assembly**

*Chullikkattil P. Pradeep, De-Liang Long, Graham N. Newton, Yu-Fei Song, and Leroy Cronin**

Polyoxometalates (POMs) are a vast class of inorganic materials derived from the early transition metals tungsten, molybdenum, and vanadium, and their assembly can bridge multiple length scales,[1,2] from the assembly of sub-nanoscale to protein sized molecules.[3] POMs have diverse physical properties[4–5] with applications in catalysis,[6] and medicine,[7] offering new approaches for the design of new materials using transferable building blocks to develop new materials.[4–7] In this respect, the use of noncovalent synthetic methodologies is attractive, as this approach is much more powerful than traditional covalent synthetic strategies.[8] It is not trivial to apply nonconvalent approaches to the design of macromolecular metal oxide structures;[2] however, predictions by Müller and Kögerler[9] and Cronin[2] suggest that this could be a unique route to develop a whole new approach to the design of molecular metal oxide architectures. We are interested in exploring the potential of weak noncovalent interactions, such as H-bonds,[10] in POM chemistry to generate a programmable route for the design and assembly of POM-based functional nanomaterials.[11] In this respect, we hypothesize that reliable generation of the hybrid building blocks in solution will allow real design.[12–14]

Herein we demonstrate that the covalent grafting of a H-bonding organic cap onto a POM cluster can control the supramolecular self-assembly of cluster species in solution and in the solid state, leading to the formation of macromolecular H-bonded nanoassemblies of polyoxometalate clusters. Most importantly, it is observed that the formation of these supramolecular architectures can be externally controlled by simply changing the grafted H-bonding organic cap and/or by changing the solvent system employed in the process. In the development of the organic–inorganic hybrid building block employed in this study, we have successfully grafted tris(hydroxymethyl)aminomethane $[(HOCH_2)_3C\text{-}NH_2$, Tris] on to a Dawson cluster, $[P_2V_3W_{15}O_{62}]^{9-}$, yielding the alkoxypolyoxometalate $(TBA)_4H_2[H_2NC(CH_2O)_3\text{-}P_2V_3W_{15}O_{59}]$, **1**·3 DMF, in good yields (Scheme 1, TBA = tetrabutylammonium cation, DMF = dimethylformamide).

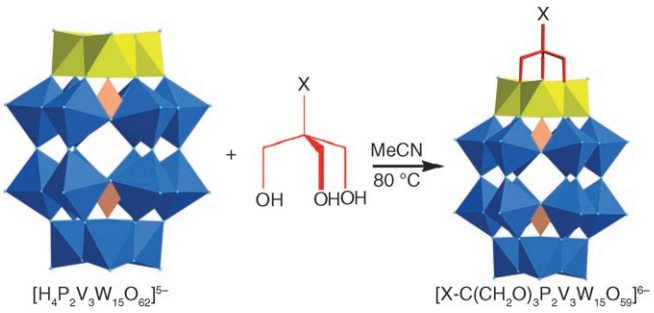

Scheme 1. Grafting Scheme of Tris derivatives to the $\{P_2W_{15}V_3\}$ cluster. VO_4 yellow, WO_4 blue, PO_4 pink. X = NH_2 (**1a**,**1b**), NO_2 (**2**), and CH_3 (**3**).

This organically grafted POM building block, **1**, is capable of forming fully H-bonded nanoassemblies not only in the solid state, but also in solution, as demonstrated by single-crystal X-ray crystallography and cryospray mass spectrometry. Furthermore, we have found that the NO_2 and CH_3-substituted derivatives of {Tris-$P_2V_3W_{15}$} clusters, compounds **2**·$CH_3CN(H_2O)_{0.5}$ and **3**·DMF, respectively assemble in different ways, as dictated by the nature of the organic cap ligand, where **2** = $(TBA)_2(C_2H_8N)_4[O_2NC(CH_2O)_3P_2V_3W_{15}O_{59}]$ (C_2H_8N is the dimethylammonium cation formed by the decomposition of DMF) and **3** = $(TBA)_4H_2[H_3CC\text{-}(CH_2O)_3P_2V_3W_{15}O_{59}]$,[15] respectively, and all these compounds have been examined using cryospray mass spectrometry and single crystal XRD[16] to assess the effect of various H-bonding tips on the grafted organic cap (NH_2, NO_2, and CH_3) in the formation of nanoassemblies.

The Tris ester (**1**) of $\{V_3\}$-capped Dawson cluster $[P_2V_3W_{15}O_{62}]^{9-}$ is synthesized as the combined H^+ and TBA salt by refluxing $(TBA)_5[H_4P_2V_3W_{15}O_{62}]$ with Tris in acetonitrile solutions in the dark, followed by ion exchange using Amberlyst 15 resin charged as the H^+ form. As a result, three bridging oxygen atoms of the $\{V_3\}$ cap of $(TBA)_5[H_4P_2V_3W_{15}O_{62}]$ cluster are replaced by the three alkoxy oxygen atoms of triol moiety giving the Tris-grafted cluster, **1**. Alkoxy POM clusters, **2** and **3**, were also synthesized following the same procedure as for the synthesis of **1**, but the triols $(HOCH_2)_3CNO_2$ (for **2**) and $(HOCH_2)_3CCH_3$ (for **3**) were used. All three compounds were characterized by elemental analyses, ^1H NMR, IR, and

[*] Dr. C. P. Pradeep, Dr. D.-L. Long, G. N. Newton, Dr. Y.-F. Song, Prof. L. Cronin
WestCHEM, Department of Chemistry
The University of Glasgow
University Avenue, Glasgow G12 8QQ (UK)
Fax: (+44) 141-330-4888
E-mail: l.cronin@chem.gla.ac.uk
Homepage: http://www.chem.gla.ac.uk/staff/lee

[**] We thank The Royal Society, EPSRC, WestCHEM and the University of Glasgow for supporting this work.

Supporting information for this article is available on the WWW under http://www.angewandte.org or from the author.

InterScience
© 2008 Wiley-VCH Verlag GmbH & Co. KGaA, Weinheim

finally by cryospray mass spectrometry and single crystal X-ray structure analysis, including bond valence sum calculations (see the Supporting Information) see Scheme 1.[17]

Crystallization of the compound **1** from acetonitrile solution by ether diffusion gave light greenish yellow block crystals, which were found to be highly hygroscopic on exposure to air. Single crystal X-ray analysis of these crystals revealed that the structure of the basic alkoxy POM anion in **1** is as expected, with the Tris moiety capping the $[P_2V_3W_{15}O_{62}]^{9-}$ cluster by replacing the three bridging μ_2-O^{2-} of the $\{V_3\}$ cap with alkoxide oxygen atoms, as shown in Scheme 1. The molecular structure of this crystal was found to be a supramolecular tetrameric structure based on **1**, having a molecular formula $(TBA)_{16}H_8[H_2NC(CH_2O)_3P_2V_3W_{15}O_{59}]_4\cdot 8(CH_3CN)$ (**1a**), $\mathbf{1}_4\cdot 8(CH_3CN)$. Each of the units **1** are connected through multiple N–H···O and C–H···O H-bonding interactions, leading to the formation of a highly distorted tetrahedral nanoassembly as shown in Figure 1. In this

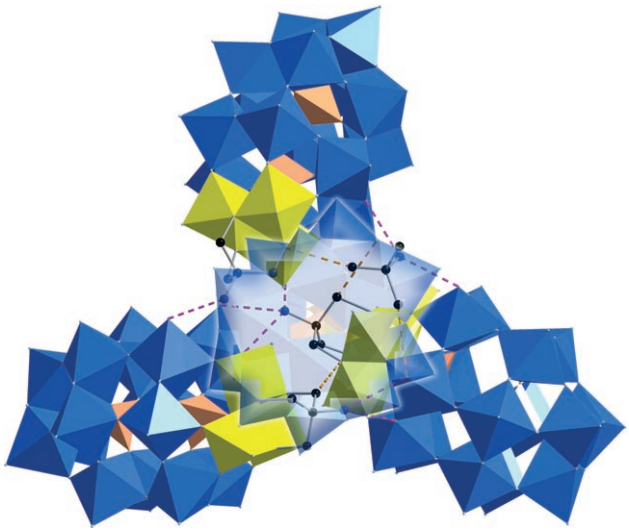

Figure 1. H-bonded distorted tetrahedral nanoassembly of the $[H_2NC(CH_2O)_3P_2V_3W_{15}O_{59}]^{6-}$ cluster in **1a**. One lobe of the tetrahedron, pointing towards the observer, is made transparent for easy visualization of the H-bonding interactions. C black, O cyan, WO_4 blue, VO_4 yellow, PO_4 pink; N–H···O interactions: purple dotted lines, C–H···O interactions: golden dotted lines.

distorted tetrahedral nanoassembly, each of the four alkoxy POM anions is connected to the other three anions through various H-bonding interactions (see the Supporting Information). The clusters are arranged such that organic cap of the cluster anions is closer to the center of the T_d (not exactly pointing to the T_d center), while the uncapped end is facing away from it. The central cavity of the T_d structure is vacant, discarding the possibility of any templating effect in the formation of such a structure. The shortest distance across the central cavity is 3.063 Å, as observed between O43 and O159. This gigantic H-bonded supermolecule has a cell volume of 101 951(4) $Å^3$.

Importantly, we were also able to isolate another supramolecular arrangement of **1**, compound **1b**, from the same crystallization experiment, although this forms in a very low yield, namely, $<10\%$. In this compound, **1b**, the structure contains chains of **1** to give **1b** as $(TBA)_4H_2[H_2NC(CH_2O)_3P_2V_3W_{15}O_{59}]\cdot 3DMF$, and uses the residual DMF present in compound **1**. Structural analysis revealed that in this crystal, the NH_2 cap of the cluster anions $[H_2NC(CH_2O)_3P_2V_3W_{15}O_{59}]^{6-}$ undergoes N–H···O interactions with another cluster (N1-O11#3 2.935(16) Å) and with two solvent DMF molecules (N1-O41#2 2.685(15), N1-O41#3 2.685(15) Å). The tetrahedral nanoassembly as observed in **1a** is not achieved in **1b** because of the H-bonding interactions of the NH_2 cap with two solvent DMF molecules instead of two cluster anions as in **1a** (Figure 2).

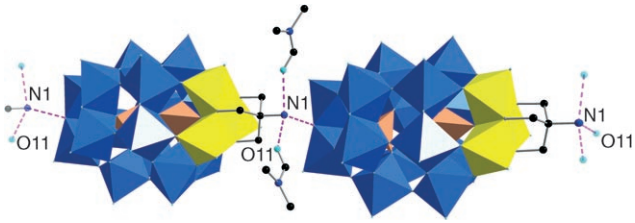

Figure 2. H-bonding interactions among $[H_2N\text{-}C(CH_2O)_3P_2V_3W_{15}O_{59}]^{6-}$ clusters in **1b** leading to chain structures in the crystal lattice. O cyan, WO_4 blue, VO_4 yellow, PO_4 pink polyhedra, N–H···O interactions: purple dotted lines.

The N–H···O interaction between the cluster units (N1-O11#3) leads to the formation of an infinite H-bonded chain structure in the crystal lattice running parallel to the *c* axis. It is interesting to note that these chains are formed purely by the interaction between alkoxy POM clusters, and no counterions or solvent molecules are involved in the formation of such chains. As the unit cell of **1b** contains two alkoxy POM clusters with their organic caps pointing opposite directions, the adjacent POM chains in the crystal lattice grow in antiparallel directions. The DMF molecules act as a glue between the neighboring chains through C–H···O interactions (C33···O3#4 3.18(3) and C31···O3 3.05(2) Å). The details of all these interactions are depicted in the Supporting Information.

The extension of the N–H···O H-bonding interactions among the POM clusters and the N–H···O and C–H···O interactions between the cluster anions and DMF molecules in three-dimensional manner leads to the formation of zigzag hydrogen bonded sheets in the crystal lattice of **1b**. These zigzag sheets are stacked one over the other in the crystal lattice, and the space between the stacks are occupied by TBA counterions (see Figures in the Supporting Information). Comparing the structures of **1b** and **1a** reveals that in **1b**, the DMF molecules present in compound **1** prevents the formation of the tetrahedral nanoassembly by undergoing H-bonding interactions with the Tris-grafted cluster anions (Figure 2). In order to prove this, we did some control crystallization experiments to investigate if the formation of tetrahedral nanoassembly **1a** is possible in the presence of DMF. These studies found that the crystallization of compound **1** in the presence of DMF in a greater concentration

 © 2008 Wiley-VCH Verlag GmbH & Co. KGaA, Weinheim

than found in the solvate of **1** (1 mM) always produces **1b**. Similarly, crystallization experiments with compound **1**, after complete removal of the DMF from **1** by thorough washing with diethyl ether, yielded only tetrameric crystals of **1a**. This demonstrates that the choice of solvent is vital for the formation hydrogen-bonded nanoassemblies, and in the case of compound **1**, it is possible to switch the supramolecular assembly from one-dimensional chains (**1b**) to the distorted tetrahedral nanocluster (**1a**) by simply changing the crystallization solvent from DMF to MeCN.

The role of the H-bonding ability of the organic cap of the cluster anions in forming the multiple aggregates of cluster species in solution and gas phase was examined by comparing the cryospray mass spectra of cluster anions $[H_2NC(CH_2O)_3P_2V_3W_{15}O_{59}]^{6-}$ (**1**), $[O_2NC(CH_2O)_3P_2V_3W_{15}O_{59}]^{6-}$ (**2**), and $[H_3CC(CH_2O)_3P_2V_3W_{15}O_{59}]^{6-}$ (**3**) under identical experimental conditions (Figure 3). By using cryospray conditions at −40 °C on compounds **1**-**3**, we were able to examine the self-assembly processes of these clusters in solution. For example, cryospray mass spectrometric studies of compound **1** in dilute acetonitrile solutions revealed that the Tris-grafted POM cluster exists in the solution phase as monomers, dimers, trimers, and even the tetramer could also be clearly observed. Peaks associated with the monomeric species $((TBA)_4[H_2NC(CH_2O)_3P_2V_3W_{15}O_{59}]^{2-}$ and $(TBA)_5[H_2NC(CH_2O)_3P_2V_3W_{15}O_{59}]^{-})$ can be found at *m*/*z* values 2502.2 and 5247.2 respectively, the dimer $((TBA)_9[H_2NC(CH_2O)_3P_2V_3W_{15}O_{59}]_2^{3-})$ at *m*/*z* value 3416.7, and the trimer $((TBA)_{14}[H_2NC(CH_2O)_3P_2V_3W_{15}O_{59}]_3^{4-})$ at *m*/*z* 3874.5. The observed mass and charge corresponding to each of these peaks clearly matched with the assigned formulae as well as the simulated spectra. Following observations in the mass spectra of the monomer, dimer, and trimer, we were able to assign the peak at *m*/*z* 4149.5 to the tetrameric species $(TBA)_{19}[H_2NC(CH_2O)_3P_2V_3W_{15}O_{59}]_4^{5-}$. This is interesting, as this data indicates that the tetrahedral species, with a molecular mass over 21 kDa and comprising $\{W_{60}V_{12}\}$ units with 19 TBA counterions, is detected in solution. Further, the NO_2 tipped cluster **2** also forms multiple aggregates (tetramer, pentamer, and hexamer) in the gas phase. This is possible because the NO_2 group on the Tris cap causes the CH_2 groups to be acidic enough to form H-bonded interactions, whereas the CH_3-tipped cluster **3** only shows mainly monomeric and some dimeric species. This is explained by the acidity of the CH_2 groups, as shown by the NMR spectroscopy δ values of the CH_2 groups in the case of compound **2** vs. compound **3** (Figure 3). The crystallographic characterization of the tetramer with the NH_2 rather than the NO_2 tip is probably a reflection that N–H···O interactions are stronger than C–H···O interactions (these clusters can only be seen at low temperatures by cryospray mass spectrometry and not at high temperatures), as well as the NH_2-capped species being able to form head-to-head interactions resulting in a compact distorted tetrahedral structure, whereas the weaker C–H···O interactions associated with **2** could only form using head-to-tail interactions for steric reasons (see the Supporting Information). The above observations in solution and gas phase are also consistent with the observation in solid state that compound **3** crystallizes only as monomeric entities in both DMF/ether and MeCN/ether solvents, and that compound **2** crystallizes as monomeric entities from DMF/ether.

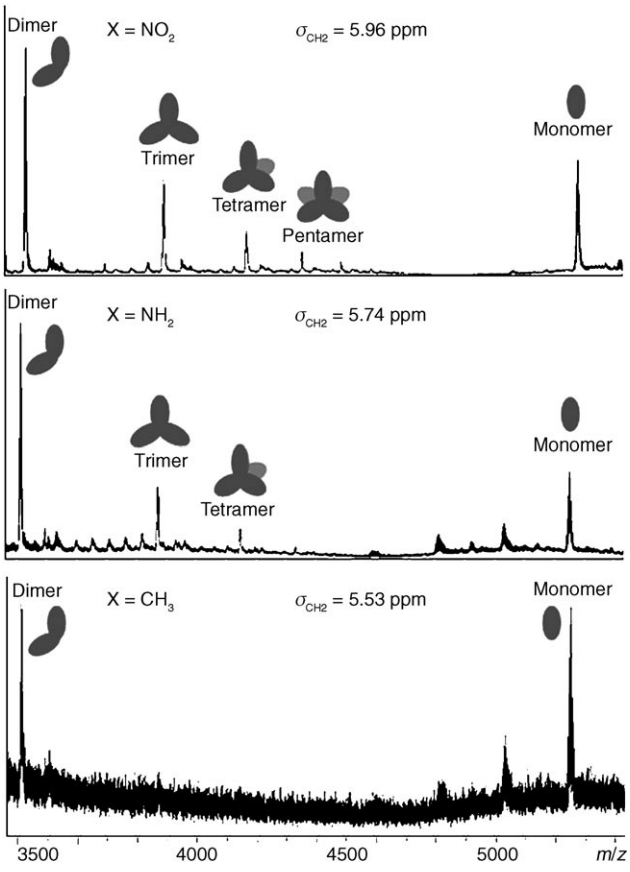

Figure 3. Comparison of the CSI-MS spectra and supramolecular assemblies of clusters **1a**, **1b** (NH_2), **2**(NO_2), and **3**(CH_3) as a function of the different substituents (X) on the organic cap, along with the chemical shift values of the CH_2 groups associated with the caps for comparison. MS Spectra are given on the same *m*/*z* scale. See the Supporting Information for the full assignment. The data are independent of concentration in the range of 10^{-7}–10^{-5} M.

These experiments also highlight the ability of weak interactions in directing the self-assembly of large cluster species in solutions leading to the formation of nanoassemblies. It can be shown that these aggregates are bound by weak interactions by increasing the energy in the collision chamber of the spectrometer. This increase in the collision energy results in rapid decrease in the dimer, trimer, and tetramer peak intensities, with an initial and simultaneous increase in monomer peak intensity. The intramonomer interactions (coordinative interactions) are more robust than the intermonomer interactions, such as H-bonding (see the Supporting Information for details of the collision energy experiments on cluster species **1** and **2**).

In summary, we have presented an approach to observe and control the hydrogen-bonded nanoassembly of polyoxometalate clusters in solid, solution, and in gas phase by covalently grafting various H-bonding organic groups on to a POM cluster. The strategy to attach an organic fragment on to a polyoxometalate to direct its supramolecular assembly resulting in ultra-large hydrogen bonded nano-architectures

 © 2008 Wiley-VCH Verlag GmbH & Co. KGaA, Weinheim

that can be observed in solution, as well as the solid state has been achieved. Most importantly, these supramolecular assemblies can be manipulated or programmed by changing the cap on the cluster and/or by changing the solvent system. The observation of the gigantic hydrogen-bonded tetrahedral nanoassembly of the alkoxy cluster anions of **1** along with 19 TBA counter ions in the solution phase by cryospray mass analysis underlines the potential of weak interactions, such as hydrogen bonding, in the design and synthesis of POM-based functional nanomaterials. In future work, we will exploit and generalize the approach given here to synthesize functional nanomaterials based upon supramolecular aggregates of polyoxometalate clusters.

Experimental Section

1: $(TBA)_5[H_4P_2V_3W_{15}O_{62}]$[18] (3.1 g, 0.6 mmol) was dissolved in 25 mL of acetonitrile. $(HOCH_2)_3CNH_2$ (Tris, 0.073 g, 0.6 mmol) was added to this solution and refluxed in the dark under N_2 atmosphere for 3 days. The resulting dark solution was added dropwise to an excess of diethyl ether with vigorous stirring, and the resulting solid was collected, reprecipitated from acetonitrile/diethyl ether, and finally dried overnight in a desiccator. The yellow precipitate was then dissolved in DMF (20 mL) and passed over a column of Amberlyst-15 ion-exchange resin (ca. 50 mL) charged in the H^+ form. The resulting solution was evaporated under reduced pressure to give a brown sticky solid which was dried under vacuum overnight, dissolved in acetonitrile (10 mL), and reprecipitated using excess diethyl ether. A light greenish–yellow precipitate was isolated by filtration and dried under vacuum to give $(TBA)_4H_2[H_2NC(CH_2O)_3P_2V_3W_{15}O_{59}]\cdot 3C_3H_7NO$. Yield: 2.1 g (0.40 mmol, 67.16%) based on $(TBA)_5[H_4P_2V_3W_{15}O_{62}]$. Elemental analysis (%) calcd for $C_{77}H_{175}N_8O_{65}P_2W_{15}V_3$ (5225.6 g mol^{-1}): C 17.70, H 3.38, N 2.14; found: C 17.85, H 3.41, N 2.24. ^{1}H NMR (400 MHz; CD_3CN): $\delta =$ 5.74 ppm (s, 6H, CH_2O), in addition to the cation and DMF resonances. FTIR (KBr): $\tilde{\nu} = 3446$, 2961, 2933, 2872, 1659, 1483, 1380, 1252, 1087, 1064, 1022, 955, 912, 816, 732, 599, 563, 529, 479. UV/Vis: 675 (22.89), 375 (5940), 315 (30200), 270 (54000).

Received: January 28, 2008
Revised: February 23, 2008
Published online: April 29, 2008

Keywords: hydrogen bonds · polyoxometalates · self-assembly · supramolecular chemistry · tungsten

[1] D.-L. Long, E. Burkholder, L. Cronin, *Chem. Soc. Rev.* **2007**, *36*, 105.
[2] D.-L. Long, L. Cronin, *Chem. Eur. J.* **2006**, *12*, 3698.
[3] A. Müller, E. Beckmann, H. Bögge, M. Schmidtmann, A. Dress, *Angew. Chem.* **2002**, *114*, 1210; *Angew. Chem. Int. Ed.* **2002**, *41*, 1162.
[4] D.-L. Long, H. Abbas, P. Kögerler, L. Cronin, *Angew. Chem.* **2005**, *117*, 3481; *Angew. Chem. Int. Ed.* **2005**, *44*, 3415; M. T. Pope, *Prog. Inorg. Chem.* **1991**, *39*, 181.
[5] A. Müller, S. Roy, *Coord. Chem. Rev.* **2003**, *245*, 153.
[6] W. B. Kim, T. Voitl, G. J. Rodriguez-Rivera, S. T. Evans, J. A. Dumesic, *Angew. Chem.* **2005**, *117*, 788; *Angew. Chem. Int. Ed.* **2005**, *44*, 778; W. B. Kim, T. Voitl, G. J. Rodriguez-Rivera, J. A. Dumesic, *Science* **2004**, *305*, 1280; B. Botar, Y. V. Geletii, P. Kögerler, D. G. Musaev, K. Morokuma, I. A. Weinstock, C. L. Hill, *J. Am. Chem. Soc.* **2006**, *128*, 11268.
[7] D. A. Judd, J. H. Nettles, N. Nevins, J. P. Snyder, D. C. Liotta, J. Tang, J. Ermolieff, R. F. Schinazi, C. L. Hill, *J. Am. Chem. Soc.* **2001**, *123*, 886.
[8] J.-M. Lehn, *Supramolecular Chemistry: Concepts and Perspectives*, VCH, Weinheim, **1995**; D. Philp, J. F. Stoddart, *Angew. Chem.* **1996**, *108*, 1242–1286; *Angew. Chem. Int. Ed. Engl.* **1996**, *35*, 1154–1196.
[9] A. Müller, P. Kögerler, *Coord. Chem. Rev.* **1999**, *182*, 3.
[10] G. A. Jeffrey, *An Introduction to Hydrogen Bonding*, Oxford University Press, New York, **1997**.
[11] P. Gomez-Romero, *Adv. Mater.* **2001**, *13*, 163; E. Coronado, C. J. Gómez-García, *Chem. Rev.* **1998**, *98*, 273.
[12] Y.-F. Song, D.-L. Long, L. Cronin, *Angew. Chem.* **2007**, *119*, 3974; *Angew. Chem. Int. Ed.* **2007**, *46*, 3900.
[13] P. R. Marcoux, B. Hasenknopf, J. Vaissermann, P. Gouzerh, *Eur. J. Inorg. Chem.* **2003**, 2406; S. Favette, B. Hasenknopf, J. Vaissermann, P. Gouzerh, C. Roux, *Chem. Commun.* **2003**, 2664; B. Hasenknopf, R. Delmont, P. Herson, P. Gouzerh, *Eur. J. Inorg. Chem.* **2002**, 1081.
[14] A. Müller, J. Meyer, H. Bögge, A. Stammler, A. Botar, *Chem. Eur. J.* **1998**, *4*, 1388; Q. Chen, D. P. Goshorn, C. P. Scholes, X. Tan, J. Zubieta, *J. Am. Chem. Soc.* **1992**, *114*, 4667.
[15] C. L. Hill et al. have carried out pioneering work in the area of alkoxy Dawson clusters. They have synthesized and characterized alkoxy POM clusters, such as $(TBA)_5H[CH_3C(CH_2O)_3V_3P_2W_{15}O_{59}]$, $(TBA)_2H_4[CH_3C(CH_2O)_3V_3P_2W_{15}O_{59}]$, $(TBA)_5H[O_2NC(CH_2O)_3V_3P_2W_{15}O_{59}]$, and $(TBA)_5H[HOCH_2C(CH_2O)_3V_3P_2W_{15}O_{59}]$; see Y. Hou, C. L. Hill, *J. Am. Chem. Soc.* **1993**, *115*, 11823. Until now, crystallographic evidence was not available showing the derivatization of the cluster.
[16] Crystal data and structure refinements for **1a**: $C_{72}H_{160}N_7O_{62}P_2V_3W_{15}$, $M_r = 5088.58$; monoclinic, $C2/c$, $a = 53.6733(12)$, $b = 35.9486(8)$, $c = 54.3715(12)$ Å, $\beta = 103.637(2)°$, $V = 101951(4)$ Å^3, $Z = 32$, 182314 reflections measured, 66466 unique, 2776 refined parameters, $R1 = 0.0856$, $wR2 = 0.1910$. **1b**: $C_{77}H_{175}N_8O_{65}P_2V_3W_{15}$, $M_r = 5225.76$; monoclinic, $P2_1m$, $a = 15.4521(3)$, $b = 21.6597(4)$, $c = 15.7896(4)$ Å, $\beta = 105.444(2)°$, $V = 5093.77(19)$ Å^3, $Z = 2$, 38137 reflections measured, 8868 unique, 477 refined parameters, $R1 = 0.0538$, $wR2 = 0.1334$. **2**: $C_{46}H_{114}N_8O_{64.5}P_2V_3W_{15}$, $M_r = 4783.96$; monoclinic, $P2_1/c$, $a = 15.7501(2)$, $b = 28.1285(4)$, $c = 22.7401(3)$ Å, $\beta = 93.503(1)°$, $V = 10055.6(2)$ Å^3, $Z = 4$, 133185 reflections measured, 18891 unique, 1300 refined parameters, $R1 = 0.0387$, $wR2 = 0.0732$. **3**: $C_{144}H_{324}N_{10}O_{126}P_4V_6W_{30}$, $M_r = 10157.15$; orthorhombic, $Pmn2_1$, $a = 23.0685(3)$, $b = 17.1276(3)$, $c = 18.7093(4)$ Å, $V = 7392.2(2)$ Å^3, $Z = 1$, 37896 reflections measured, 13554 unique, 518 refined parameters, $R1 = 0.0446$, $wR2 = 0.1237$. CCDC-675452, CCDC-675453, CCDC-675454, and CCDC-675455 contain the supplementary crystallographic data for this paper. These data can be obtained free of charge from The Cambridge Crystallographic Data Centre via www.ccdc.cam.ac.uk/data_request/cif.
[17] The basic alkoxy POM clusters in **2**, $[O_2NC(CH_2O)_3V_3P_2W_{15}O_{59}]^{6-}$, and **3**, $[CH_3C(CH_2O)_3V_3P_2W_{15}O_{59}]^{6-}$, are same as reported by Craig Hill et al. The only difference is in the counterions, which may be due to the slight difference in the experimental procedures.
[18] R. G. Finke, B. Rapko, R. J. Saxton, P. J. Domaille, *J. Am. Chem. Soc.* **1986**, *108*, 2947.

 © 2008 Wiley-VCH Verlag GmbH & Co. KGaA, Weinheim